KTH Machine Design

Airborne Wear Particles Emissions from Commercial Disc Brake Materials
– Passenger Car Field Test

Jens Wahlström, Ulf Olofsson, Anders Jansson and Lars Olander

Department of Machine Design
Royal Institute of Technology
SE-100 44 Stockholm

TRITA – MMK 2008:21
ISSN 1400-1179
ISRN/KTH/MMK/R-08/21-SE

1 Abstract

Most modern passenger cars have disc brakes on the front wheels, which unlike drum brakes are not sealed off to the ambient air. During braking, there is wear to both the rotor and the pads. This wear process generates particles, which may become airborne. In field tests it is difficult to distinguish these particles from others in the surrounding environment. It may be preferable to use laboratory test stands where the cleanness of the surrounding air can be controlled. The validity of these test stands has to be verified by comparison with field tests and therefore a test series has been conducted. These tests were performed in Stockholm, Sweden, in urban traffic. Low metallic type brake pads and gray cast iron rotors were tested. The results indicate that this test methodology can be used to study the number and mass concentrations as well as size distributions of particles generated from car disc brakes. Overall, the measured mean particle number and mass diameters of the airborne particles were 0.39 μm and 1.5 μm, respectively.

Key words: wear, airborne particles, disc brake, field test

2 Table of content

3 Introduction

Several studies have shown an association between adverse health effects and the concentration of airborne particles in the atmosphere [1–3]. In urban environments, airborne particles can come from different sources, for example, demolition and construction [4], resuspended road dust [5], wheel-to-rail contact [6, 7], car-to-road contact [8, 9], and disc brakes [10, 11]. During braking both the rotor and the pads are worn and this process generates wear particles, some of which become airborne. Limit levels for PM_{10} (airborne particles with an aerodynamic diameter smaller than 10 μm) is set in EU by the EC (European Commission) and in U.S. the limit levels for PM_{10} are set by the EPA (Environmental Protection Agency). In this technical report the focus is on airborne wear particles. However, wear particles from disc brakes also have an esthetical influence because some of them get stuck on the visible surfaces of the wheel rims.

The wear particles originate from the rotors and the pads. Most rotors used in passenger cars are made of grey cast iron. The brake pads can be made of many different material compositions [12]. Essentially, brake pads are of three types: non-asbestos organic (NAO), semi-metallic and low metallic. According to [10] the NAO type brake pads have a relatively low brake noise and low wear rates but lose braking capacity during high temperature. Semi-metallic type brake pads have a high steel fibre and iron powder content and low wear but are noisier than the other pad types. Low metallic type of brake pads have a relative high content of abrasives which results in a high friction and a good braking capacity at high temperatures. In the present work a grey cast iron rotor and low metallic pads are tested.

When measuring airborne brake wear particles in field tests, it can be difficult to distinguish these from others in the surrounding environment, that is, from other traffic-generated aerosols. Although several studies have been focused on the study of wear and friction at the pad to rotor interface in laboratory test stands, few of them [13, 14] have focused on online measurements of airborne wear particles. Also, passenger car field tests are rare. Sanders et al [10] measured particle and mass concentrations of airborne particles in a field test and compared the results with those measured in dynamometer tests. Wahlström et al. [15] measured number and mass concentration of airborne particles in a field test and made comparisons with results from a pin-on-disc test stand and from a disc brake assembly test stand. The representativity of the test stand measurements should be verified by comparison with field tests and therefore a field test series was conducted. The purpose of this technical report is to describe and present the results from these field tests in Stockholm, Sweden.

4 Experimental setup

A passenger car was used in this field test. A brake corner at the front wheel in this passenger car consists of a knuckle, the wheel bearing, and the disc brake assembly. The disc brake assembly in turn consists of a ventilated rotor, a sliding calliper with a single piston, and two brake pads (see Figure 1). The finger side brake pad includes a K-type thermocouple that measures the temperature near the finger side pad-to-rotor contact. The pads used in this brake corner are made of low metallic material and the rotor is made of grey cast iron. The speed of the car is measured by a built-in Hall effect sensor in the wheel bearing, with 48 pulses per revolution. The signals from the speed sensor and the pressure sensor are connected to an HBM Spider 8 amplifier, which in turn is connected to a computer for storage of the measured data.

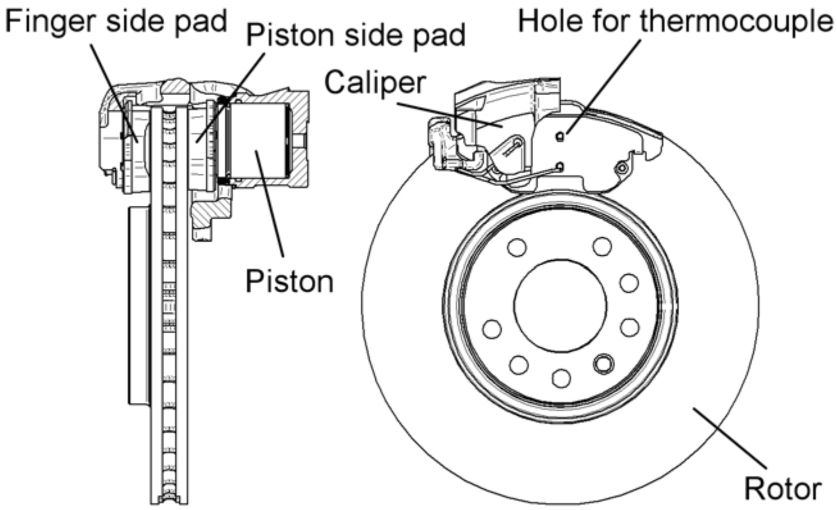

Figure 1. Disc brake assembly with a single piston floating caliper and a ventilated rotor.

The car was prepared with four particle instruments which measured particle concentrations. Two test tubes were mounted near the outlet of the front right disc brake (see Figure 2) and two test tubes were mounted in the front of the car (see Figure 3). The concentrations of airborne particles near the outlet of the brake were measured online during the test runs by a GRIMM [16] optical counter and a DustTrak photometer. Connected to the tubes in the front of the car another GRIMM and DustTrak registered the background concentrations. GRIMM is an optical particle counter (light scattering) called Aerosol Spectrometer, which measures airborne particles from 0.25 μm to 32 μm in 31 size intervals and concentrations from 1 particle/dm^3 to $2 \cdot 10^6$ particles/dm^3 with a sample flow rate of 72 l/h (0.02 l/s). The particle concentration is stored every sixth second. An optical particle counter is sensitive to the shape and refractive index of the particles, which means that the measured particle sizes and thus number distributions are approximate [17]. The DustTrak is a photometer which reports the mass concentration in mg/m^3. This instrument is also of type light scattering and can measure particle concentrations corresponding to respirable size, PM10, PM2.5 or PM1.0 size fraction. It was used without pre-precipitator in these experiments and then measured particles between 0.1 and 10 μm. The instrument is calibrated with a standardized test dust, which has a different size distribution, density and refractive index than the here measured particles. Thus the output from this instrument can only be used as a relative measure, but is useful to register changes in time of generated particle mass [18].

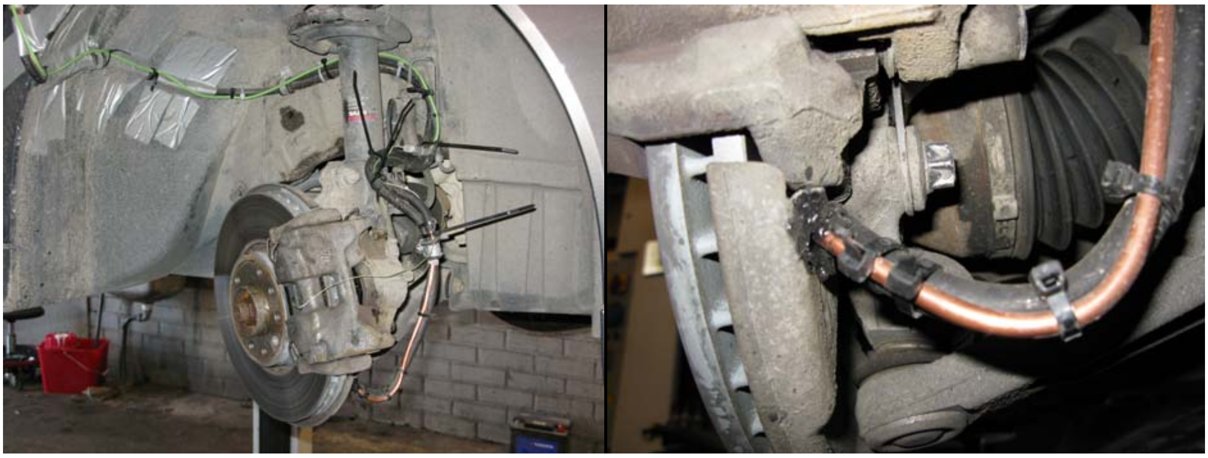

Figure 2. Photo of the test tubes for particle measurements mounted directly after the piston side brake pad on the piston side.

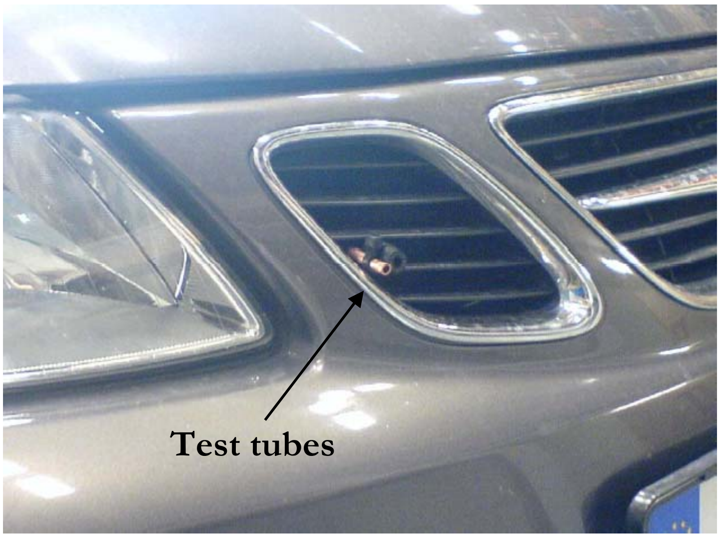

Figure 3. Photo of the test tubes for measurements of the background particle concentration mounted in the front of the test car.

5 Test procedure

Five test runs was performed on a test track (see Figure 4) in Stockholm, Sweden. To purpose of this test track was to simulate urban driving. It contains one part of country roads were the traffic flow is relative low and the mean speed of the car was around 30 km/h and one part of highway were the traffic flow is higher. To reduce the influence of re-suspended, traffic generated particles in the background, two of the tests were conducted at night time with low traffic. Three tests were conducted at day time when it rained to minimize particle re-suspension from traffic.

Each test run took about 17 minutes. During the test runs, the brake cylinder pressure and the car speed were measured with a sampling frequency of 1200 Hz. The finger side pad temperature was sampled at 3 Hz. The particle concentrations were stored every six seconds. The particle instruments were switched between each test, i.e. the instruments used for the front were used for the brake in next test run, and vice versa.

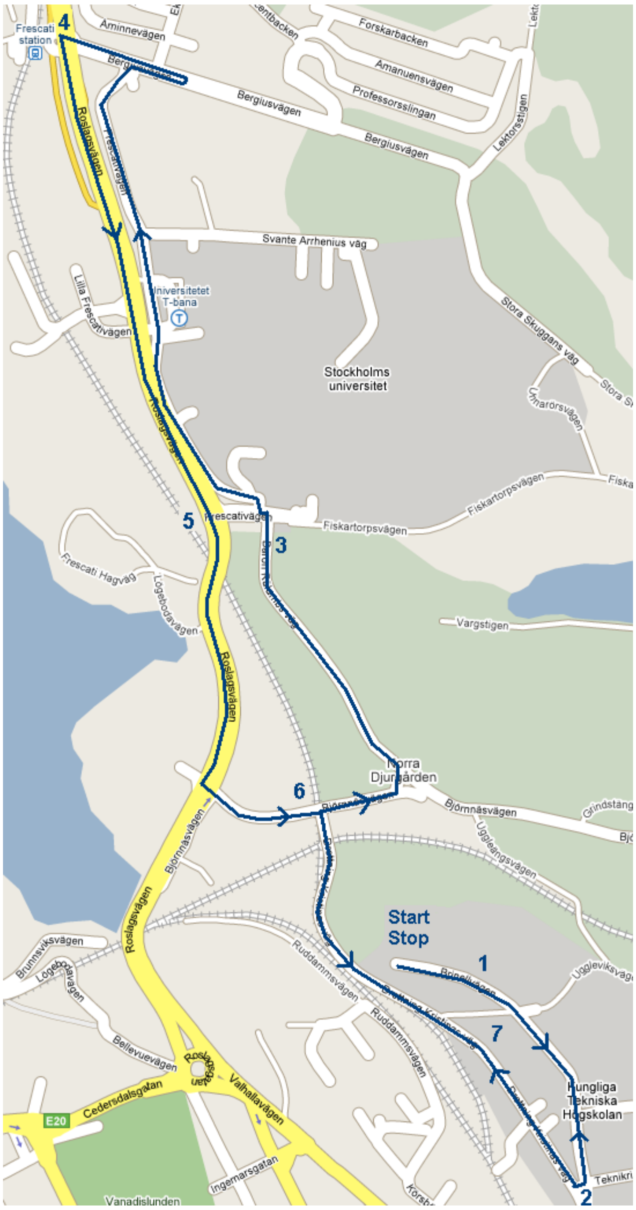

Figure 4. Map of the test track in Stockholm, Sweden. The yellow marked road is high ways (≈ 70 km/h) and the white marked road is country roads (≈ 30 km/h). Test track conditions; 1: Weak downhill slope. 2: Country road intersection. 3: Country road intersection. 4: Slipway on to high way. 5: Highway intersection with traffic light. 6: Country road intersection. 7: Weak downhill slope.

6 Results

The results from the field test are presented in sections 6.1 to 6.5. For simplicity, the measured particle concentrations are divided into a coarse particle fraction (particles with measured diameters between 1 µm and 32 µm) and a fine particle fraction (particles with measured diameters lesser than 1 µm).

In Figure 7, Figure 11, Figure 15, Figure 19, and Figure 23 the maximum normalized fine fraction particle concentrations as measured by the GRIMM instrument, brake cylinder pressure and car speed are presented.

In Figure 8, Figure 12, Figure 16, Figure 20, and Figure 24 the maximum normalized coarse fraction particle concentrations as measured by the GRIMM instrument, brake cylinder pressure and car speed are presented.

The measured mass and particle concentration near the disc brake and in the background can be seen in Figure 9, Figure 13, Figure 17, Figure 21 and Figure 25. Note that the background particle concentration as measured with the GRIMM instrument is small relative to the particle concentration near the brake. The measured background mass concentration can also be distinguished from the mass concentration near the brake.

The measured brake cylinder torque, finger side pad temperature and car speed can be seen in Figure 10, Figure 14, Figure 18, Figure 22, and Figure 26.

Characteristic particle and volume size distributions corrected for the background concentrations in the front of the car during the tests are presented in Figure 5 and Figure 6. The characteristic particle and volume concentrations were calculated between different times for different test runs, see Table 1. These time intervals were chosen for periods when the particle concentration increased after an increase in cylinder brake pressure.

In Table 2 the particle and volume concentrations used for normalization of the particle and volume size distributions are presented. Note that all tests have a maximum peak in the mean particle size concentration, in the fine fraction, between 0.35 µm and 0.5 µm. Table 3 presents the particle and volume-weighted mean diameter for each test run and an overall mean and standard deviation. Also, most of the particles generated are in the fine fraction. In Table 4 the mean particle and mass concentration measured in the front of the car is presented and in Table 5 is the mean particle and mass concentration measured near the brake presented.

Table 1. Time intervals to calculate the characteristic normalized size distribution for the different test runs.

	Interval 1 [min]	Interval 2 [min]
Night run 1	7-9	14-17
Night run 2	3-4	5-6

Day run 1	5-6	13-16.5
Day run 2	1-2	3-4
Day run 3	1-4	5-7

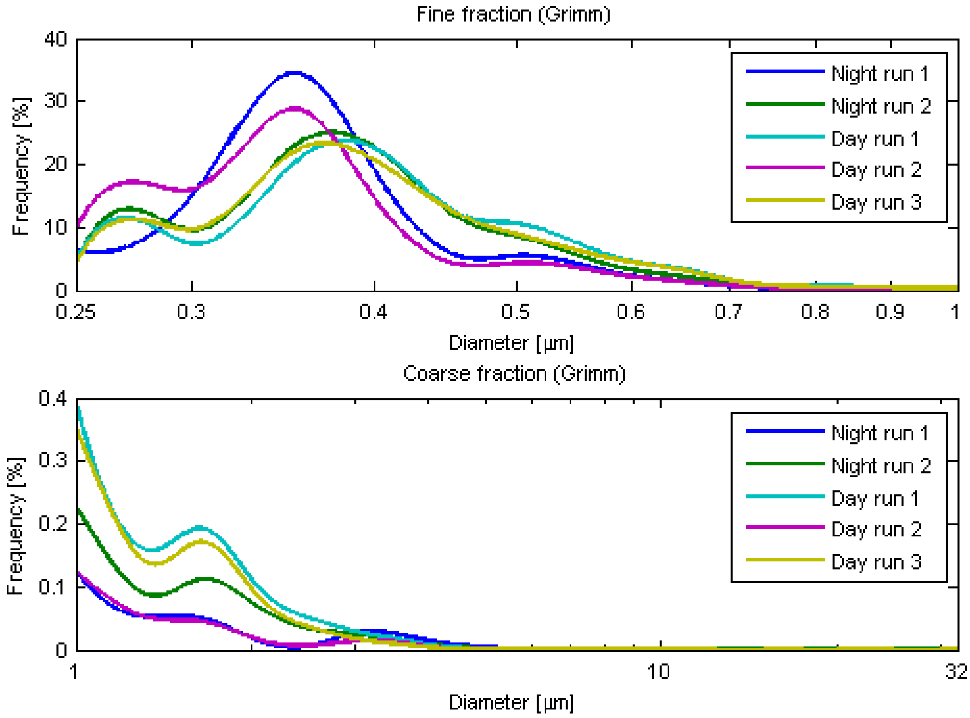

Figure 5. Mean normalized particle size distributions as measured with the GRIMM instrument.

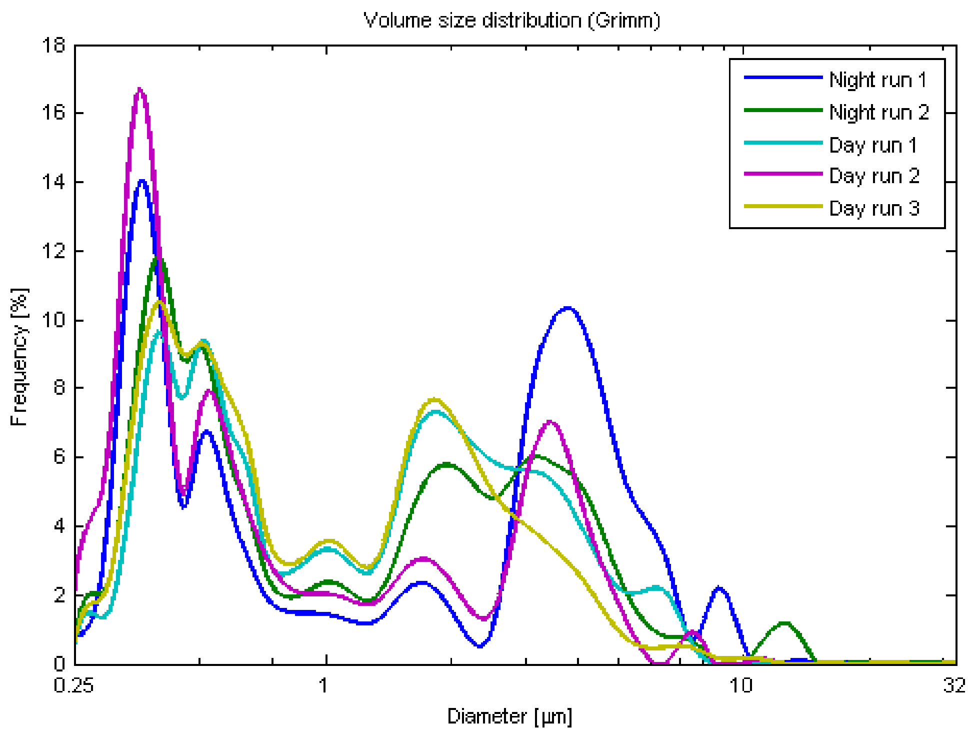

Figure 6. Mean normalized volume size distributions as measured with the GRIMM instrument.

Table 2. The particle and mass concentrations used for normalization of the particle and volume size distributions.

	Night run 1	Night run 2	Day run 1	Day run 2	Day run 3
Particle conc. [10^6 no./m^3]	4	9	6	10	24
Mass conc. [10^6 mg/m^3]	0.3	0.7	0.5	0.5	1.9

Table 3. The number and volume-weighted mean diameter for each test run and the overall mean and standard deviation.

	Night run 1	Night run 2	Day run 1	Day run 2	Day run 3	Mean	Std
Number weighted [µm]	0.37	0.40	0.42	0.36	0.41	0.39	0.03
Vol. weighted[µm]	2.1	1.6	1.5	1.2	1.2	1.5	0.35

Table 4. The mean mass and particle concentration as measured with the DustTrak and Grimm instrument in the front of the car.

	Night run 1	Night run 2	Day run 1	Day run 2	Day run 3
DustTrak [mg/m^3]	0.0139	0.0123	0.0062	0.0109	0.0058
Grimm [10^6 no./m^3]	52	40	23	30	21

Table 5. The mean mass and particle concentration as measured with the DustTrak and Grimm instrument near the brake.

	Night run 1	Night run 2	Day run 1	Day run 2	Day run 3
DustTrak [mg/m^3]	0.0180	0.0242	0.0151	0.0284	0.0528
Grimm [10^6 no./m^3]	265	491	325	551	1252

6.1 Night run 1 (2008-08-26)

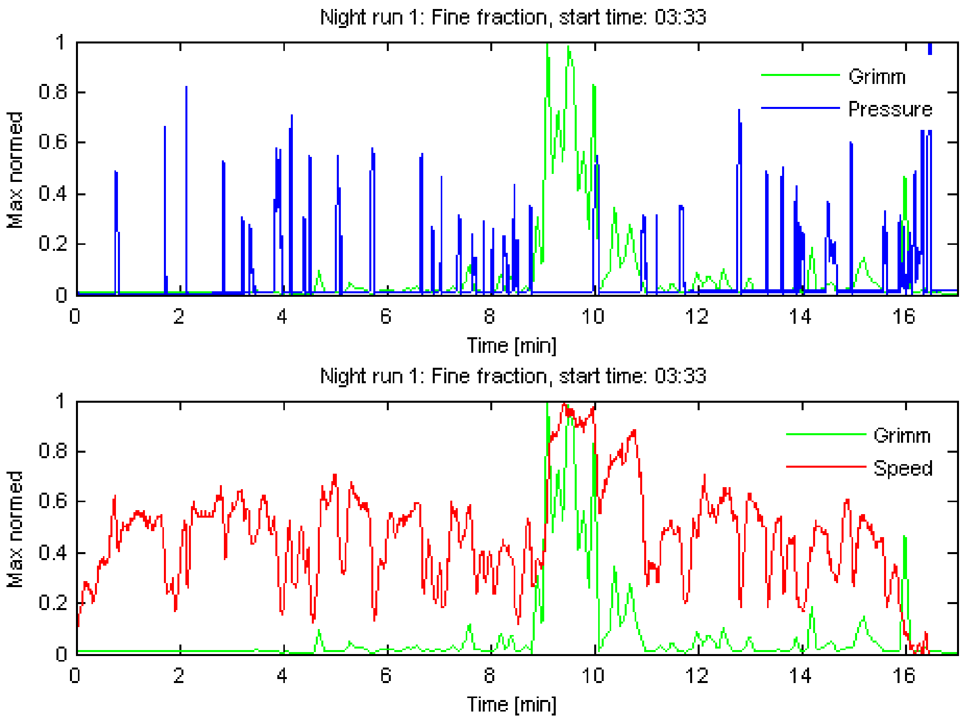

Figure 7. The green graph is the fine fraction particle concentrations as measured by the GRIMM instrument, the blue graph is the measured brake cylinder pressure, and the red graph is the measured speed of the car.

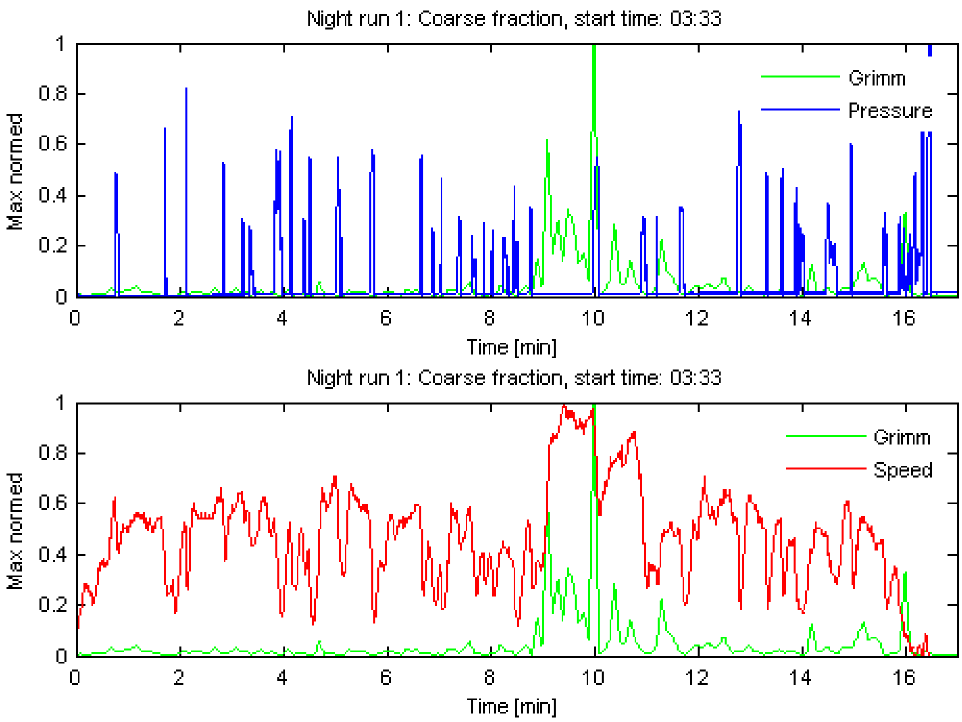

Figure 8. The green graph is the coarse fraction particle concentrations as measured by the GRIMM instrument, the blue graph is the measured brake cylinder pressure, and the red graph is the measured speed of the car.

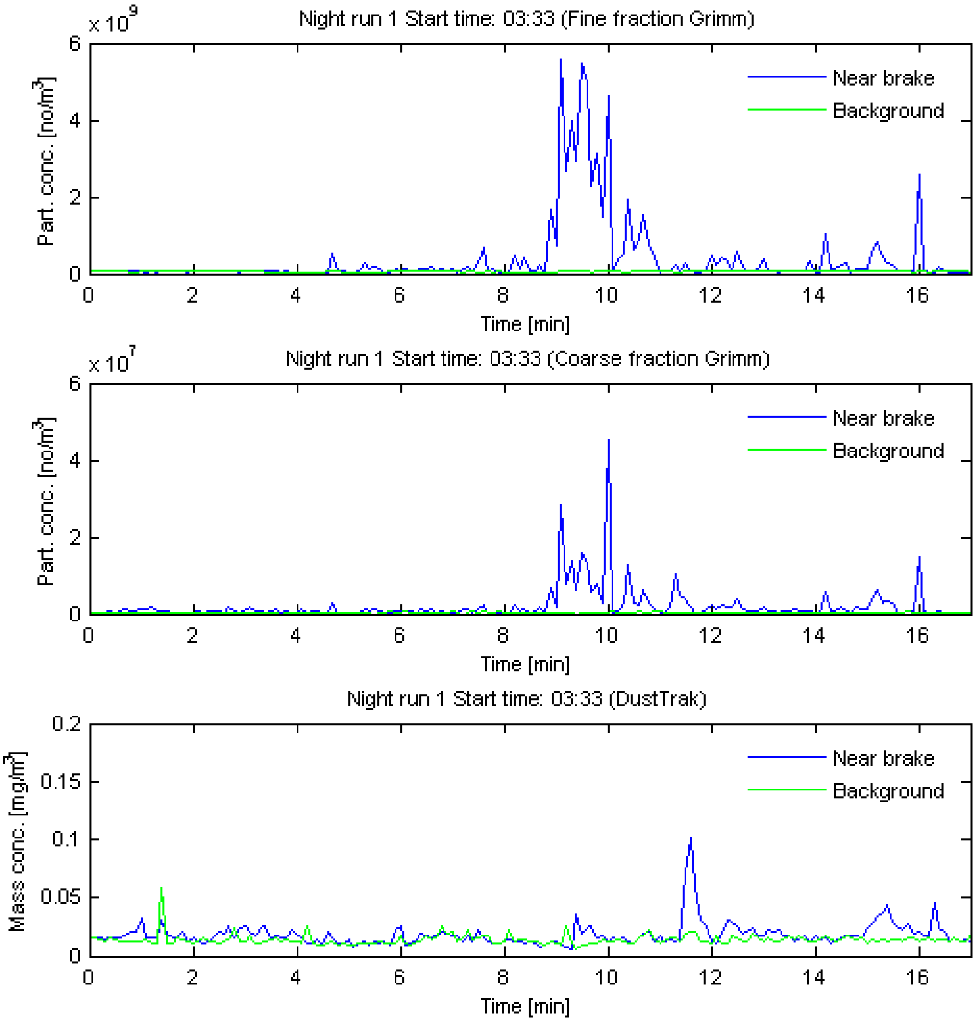

Figure 9. Fine and coarse fraction particle concentrations as measured by the GRIMM instrument during the test time and the mass concentration as measured by the DustTrak instrument. The blue graphs are the concentrations measured near the brake and the green graphs are the measured background concentration.

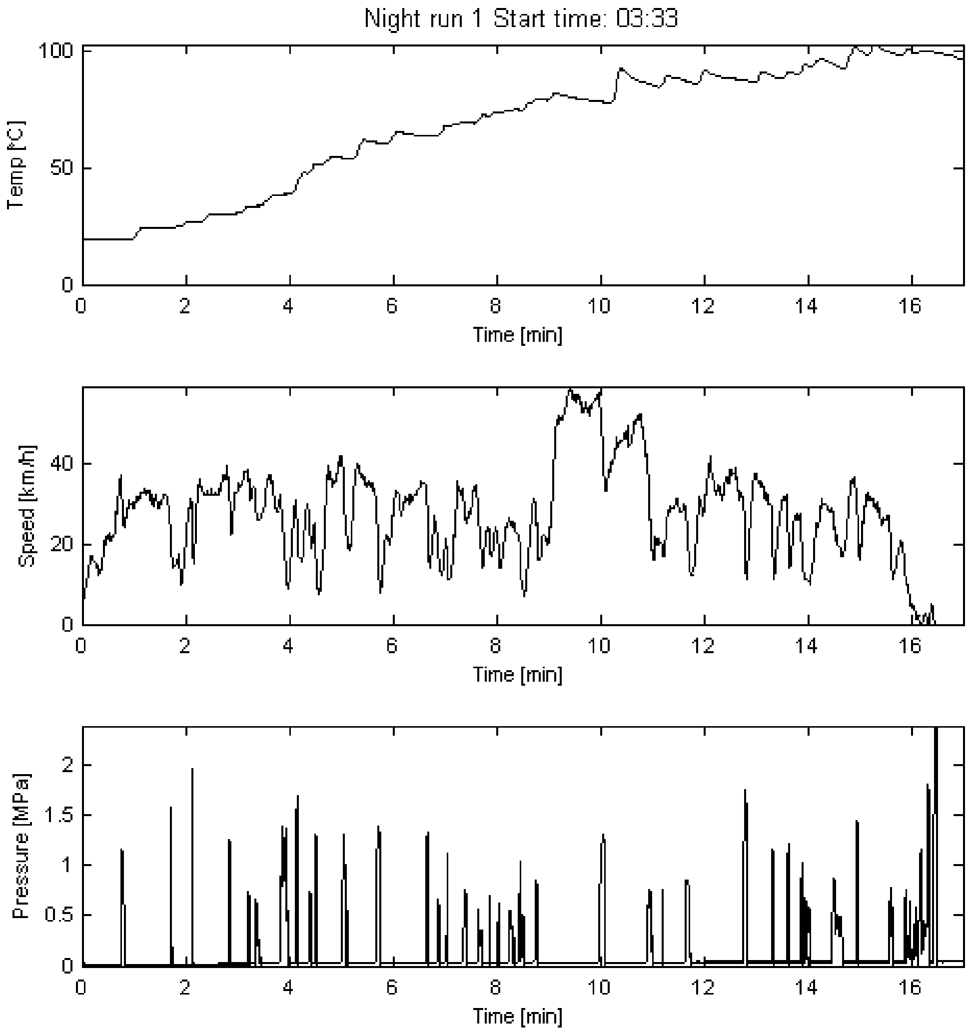

Figure 10. Finger side pad temperature, car speed and brake cylinder pressure measured during the test run.

6.2 Night run 2 (2008-08-26)

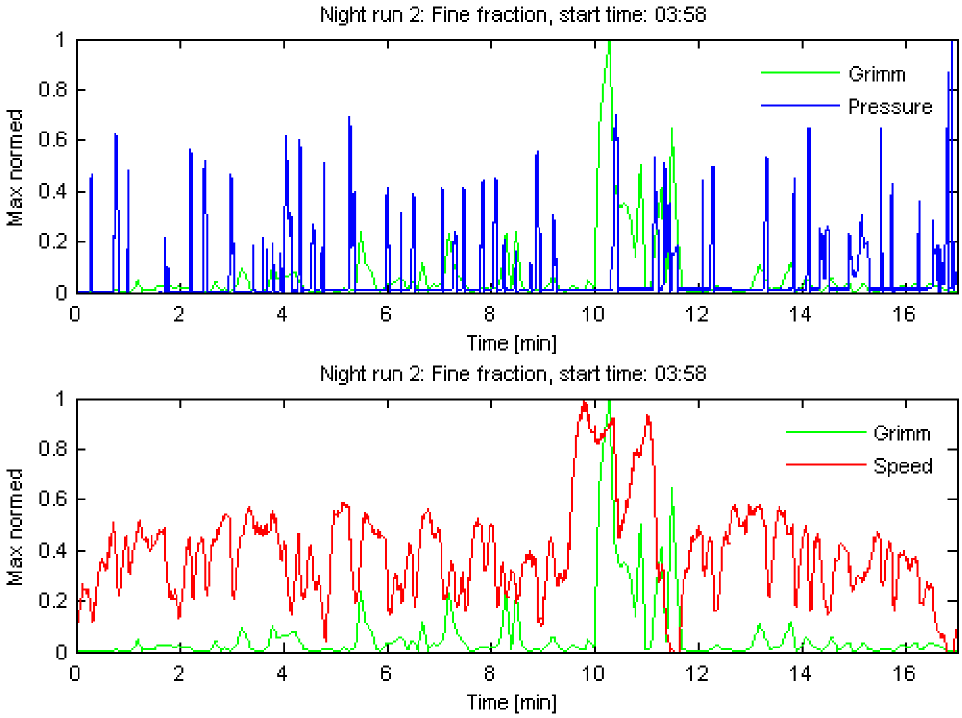

Figure 11. The green graph is the fine fraction particle concentrations as measured by the GRIMM instrument, the blue graph is the measured brake cylinder pressure, and the red graph is the measured speed of the car.

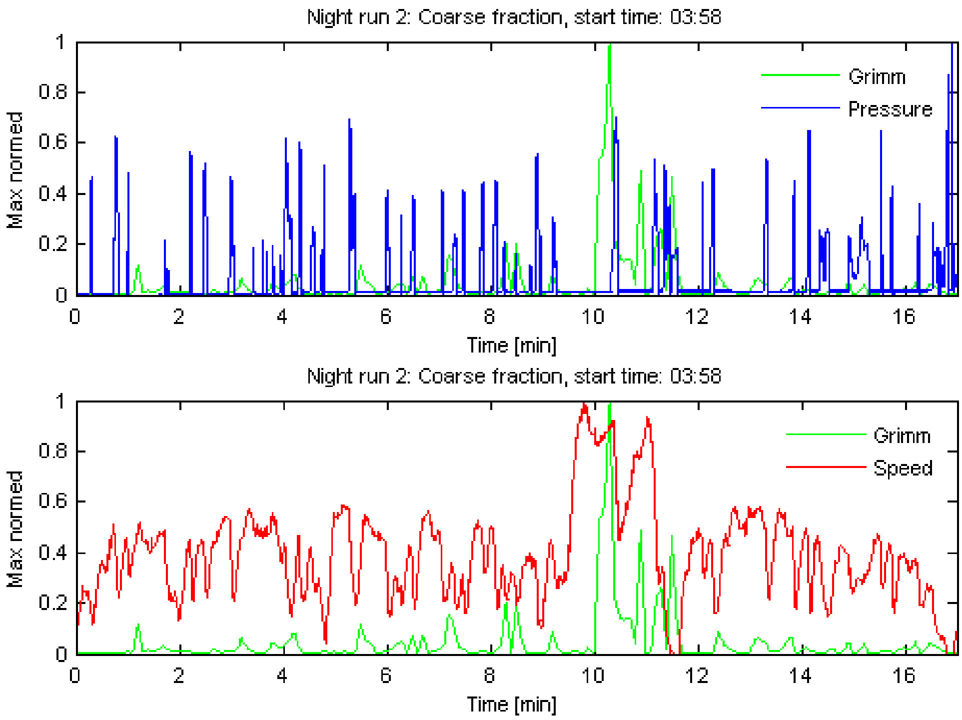

Figure 12. The green graph is the coarse fraction particle concentrations as measured by the GRIMM instrument, the blue graph is the measured brake cylinder pressure, and the red graph is the measured speed of the car.

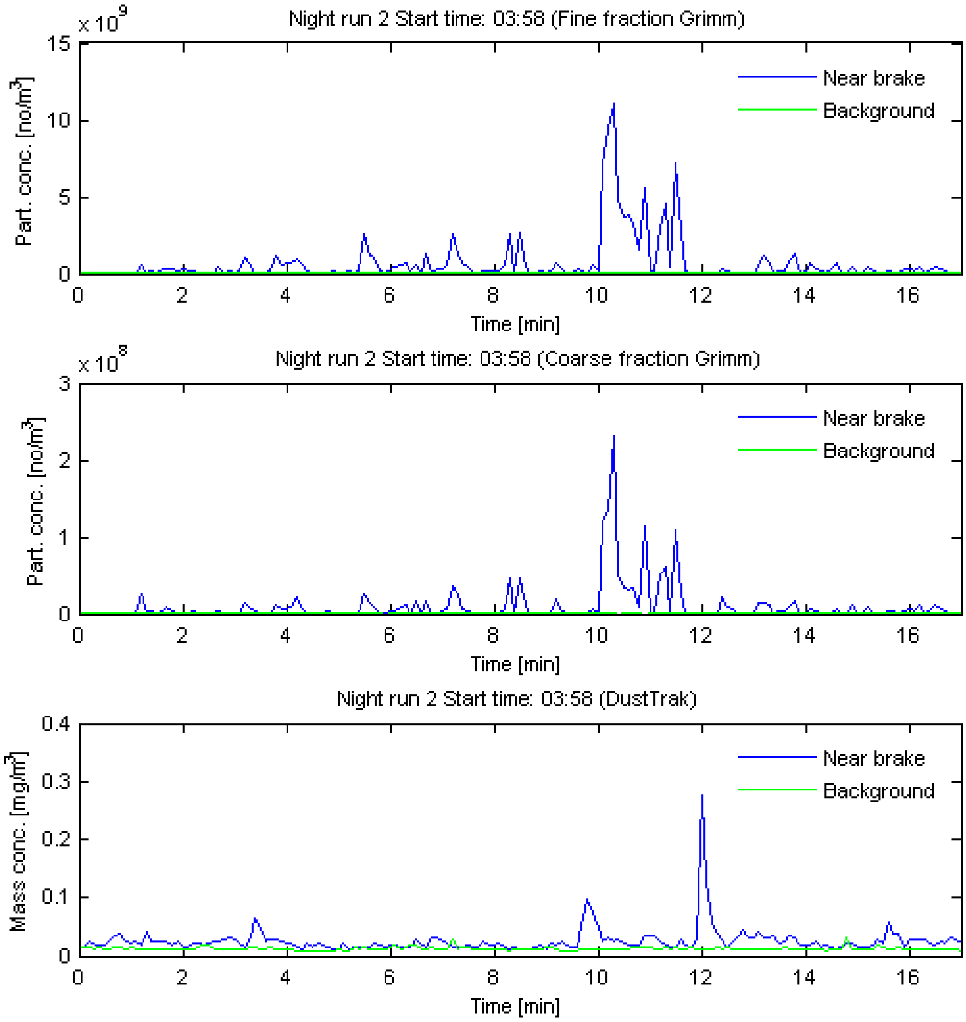

Figure 13. Fine and coarse fraction particle concentrations as measured by the GRIMM instrument during the test time and the mass concentration as measured by the DustTrak instrument. The blue graphs are the concentrations measured near the brake and the green graphs are the measured background concentration.

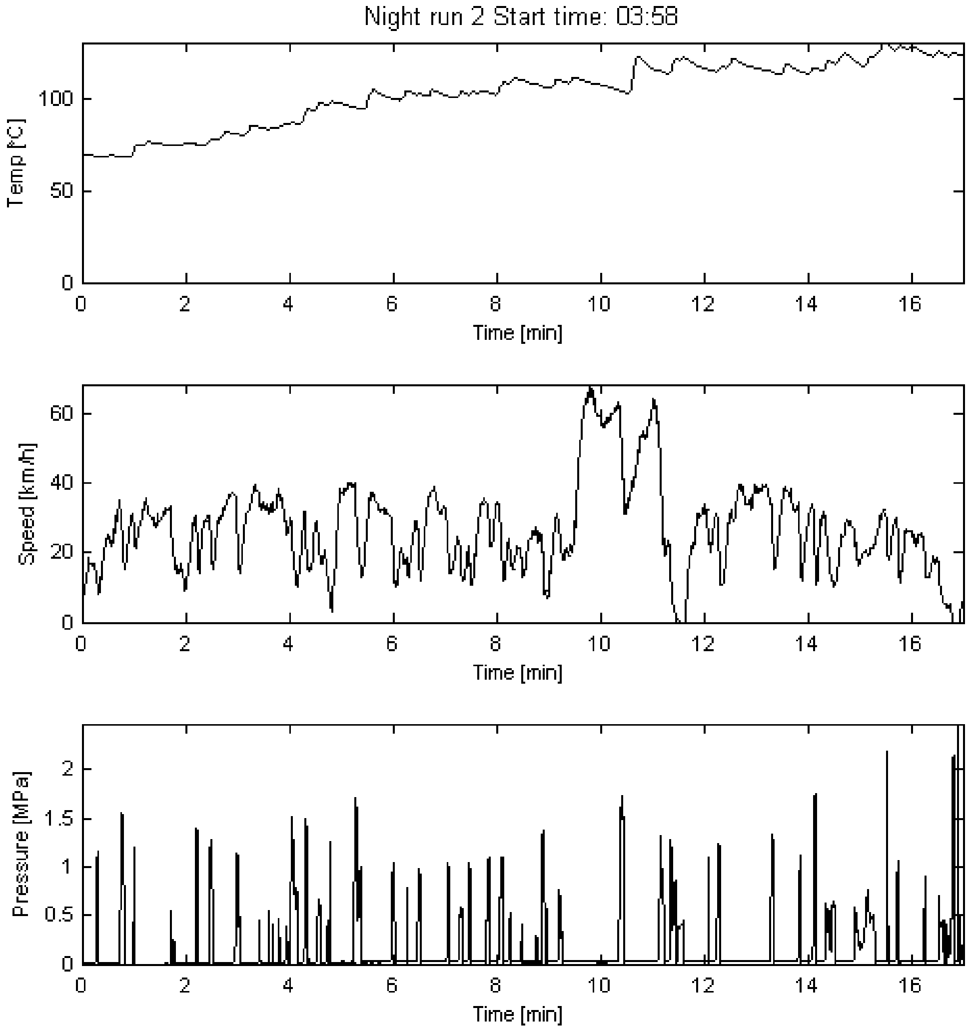

Figure 14. Finger side pad temperature, car speed and brake cylinder pressure measured during the test run.

6.3 Day run 1 (2008-08-28)

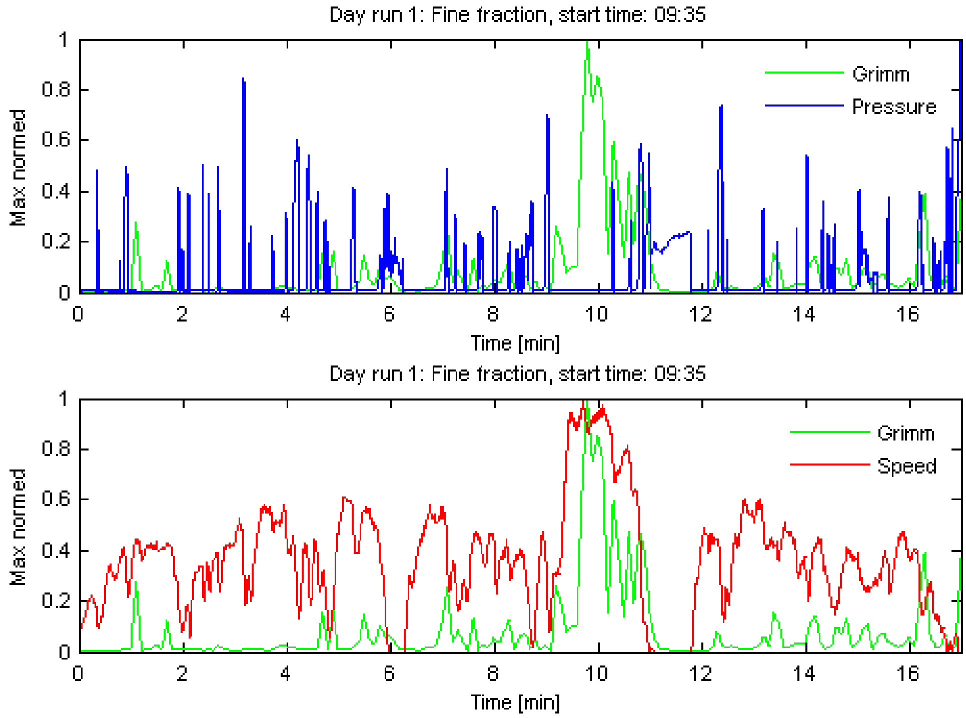

Figure 15. The green graph is the fine fraction particle concentrations as measured by the GRIMM instrument, the blue graph is the measured brake cylinder pressure, and the red graph is the measured speed of the car.

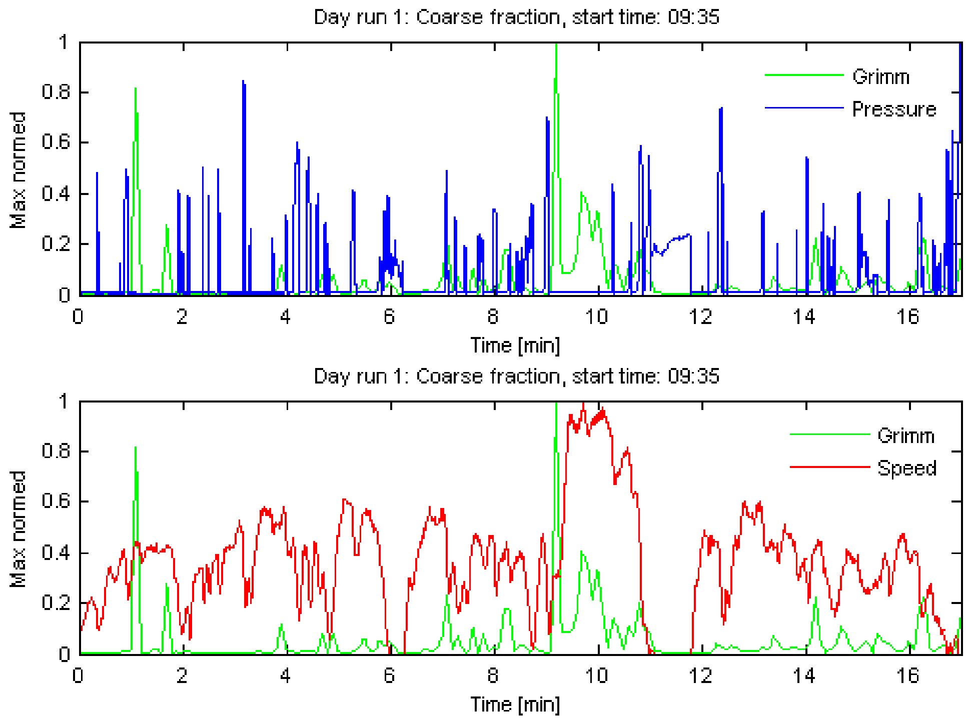

Figure 16. The green graph is the coarse fraction particle concentrations as measured by the GRIMM instrument, the blue graph is the measured brake cylinder pressure, and the red graph is the measured speed of the car.

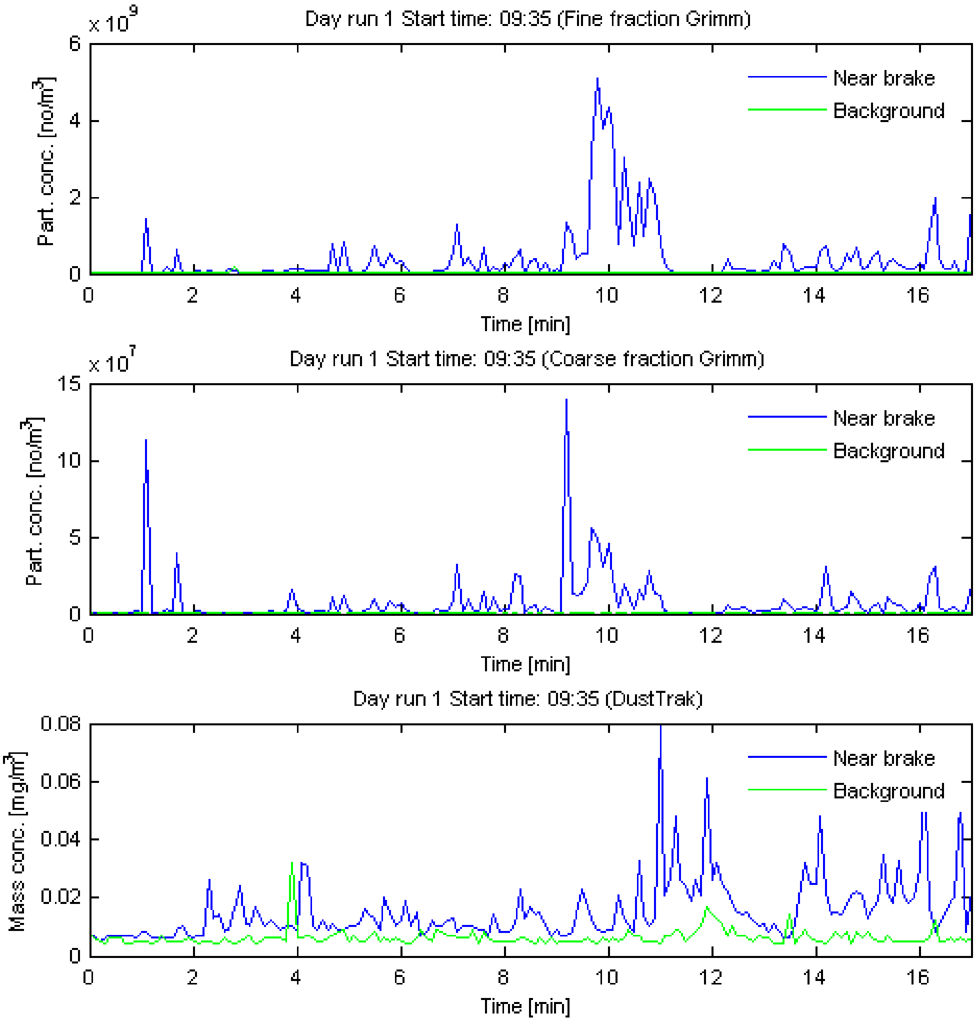

Figure 17. Fine and coarse fraction particle concentrations as measured by the GRIMM instrument during the test time and the mass concentration as measured by the DustTrak instrument. The blue graphs are the concentrations measured near the brake and the green graphs are the measured background concentration.

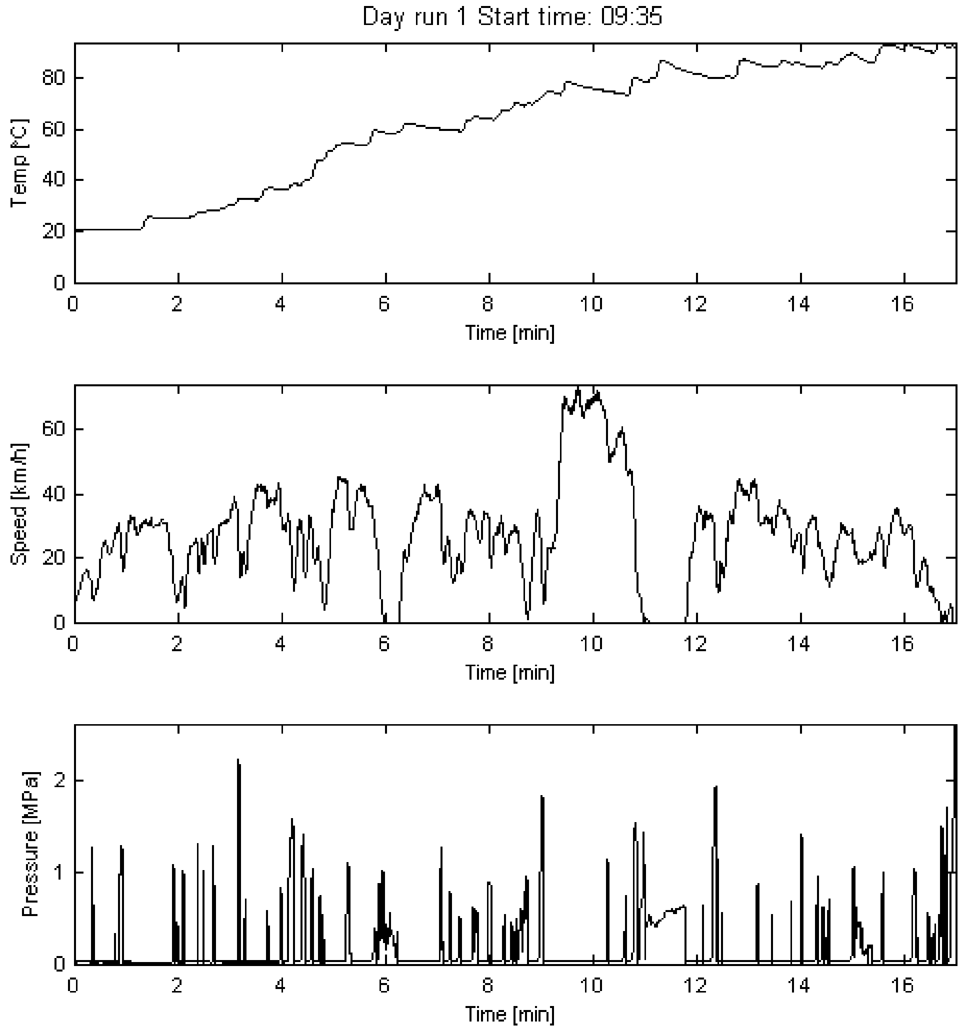

Figure 18. Finger side pad temperature, car speed and brake cylinder pressure measured during the test run.

6.4 Day run 2 (2008-08-28)

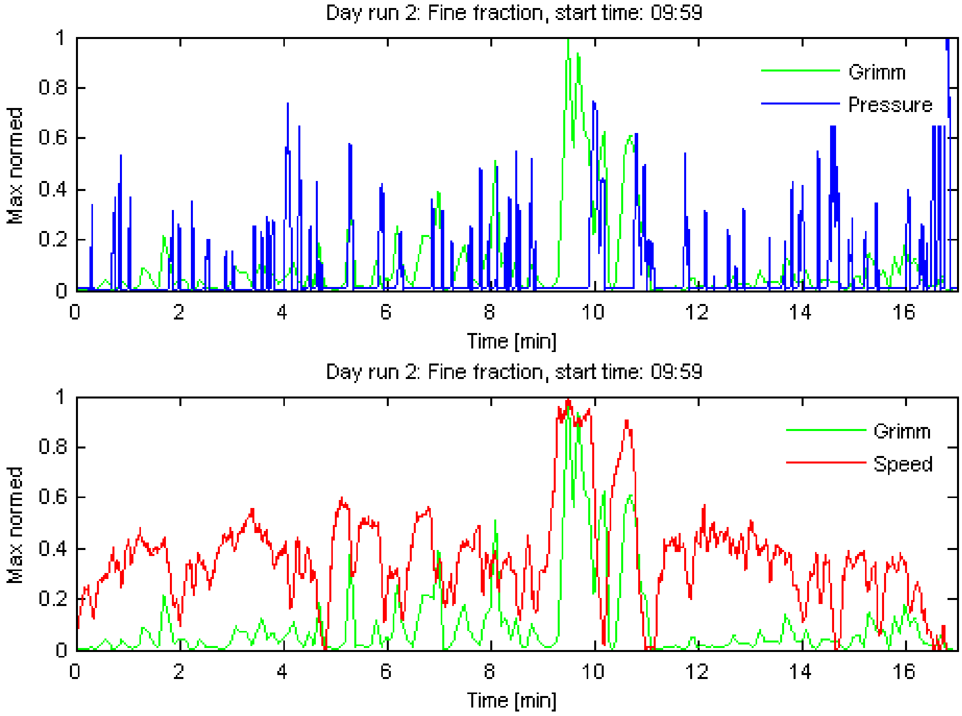

Figure 19. The green graph is the fine fraction particle concentrations as measured by the GRIMM instrument, the blue graph is the measured brake cylinder pressure, and the red graph is the measured speed of the car.

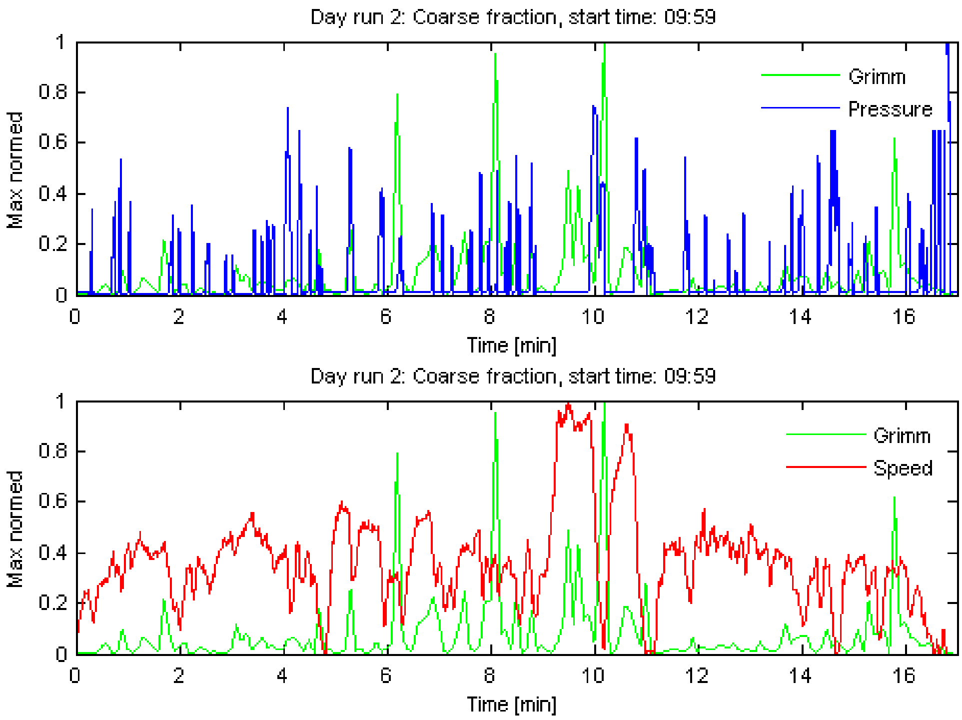

Figure 20. The green graph is the coarse fraction particle concentrations as measured by the GRIMM instrument, the blue graph is the measured brake cylinder pressure, and the red graph is the measured speed of the car.

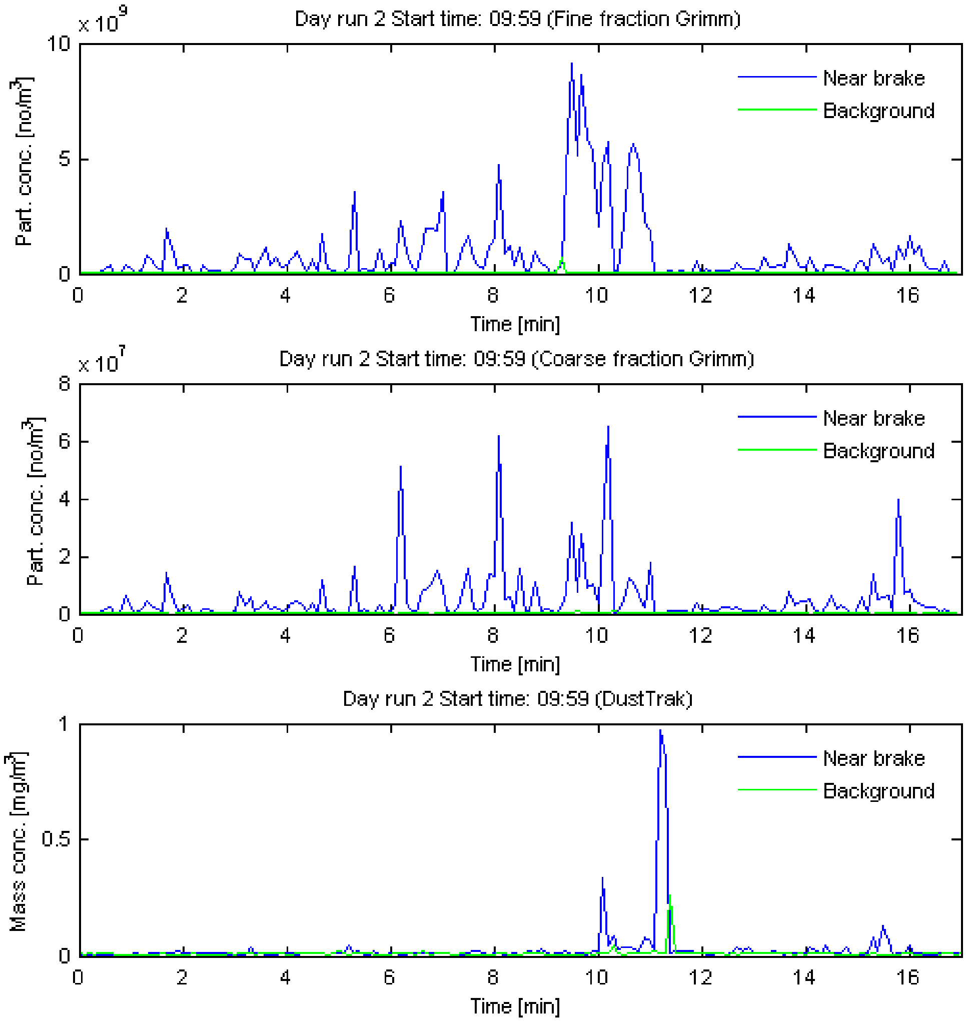

Figure 21. Fine and coarse fraction particle concentrations as measured by the GRIMM instrument during the test time and the mass concentration as measured by the DustTrak instrument. The blue graphs are the concentrations measured near the brake and the green graphs are the measured background concentration.

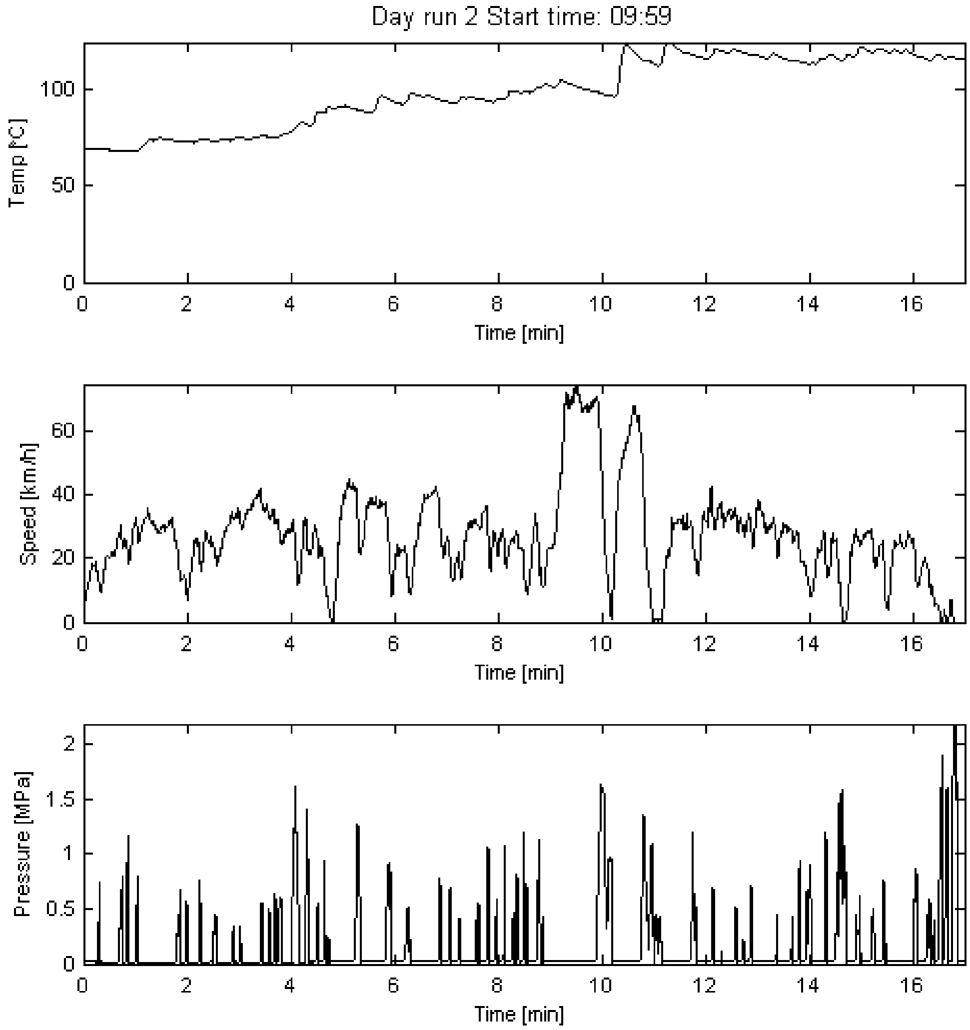

Figure 22. Finger side pad temperature, car speed and brake cylinder pressure measured during the test run.

6.5 Day run 3 (2008-08-28)

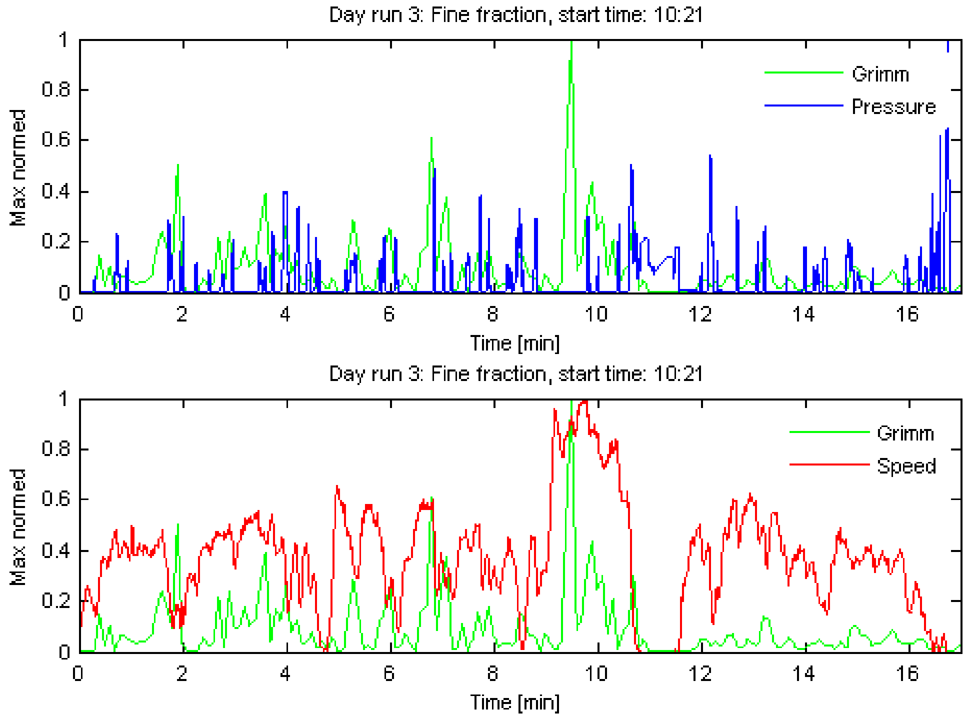

Figure 23. The green graph is the fine fraction particle concentrations as measured by the GRIMM instrument, the blue graph is the measured brake cylinder pressure, and the red graph is the measured speed of the car.

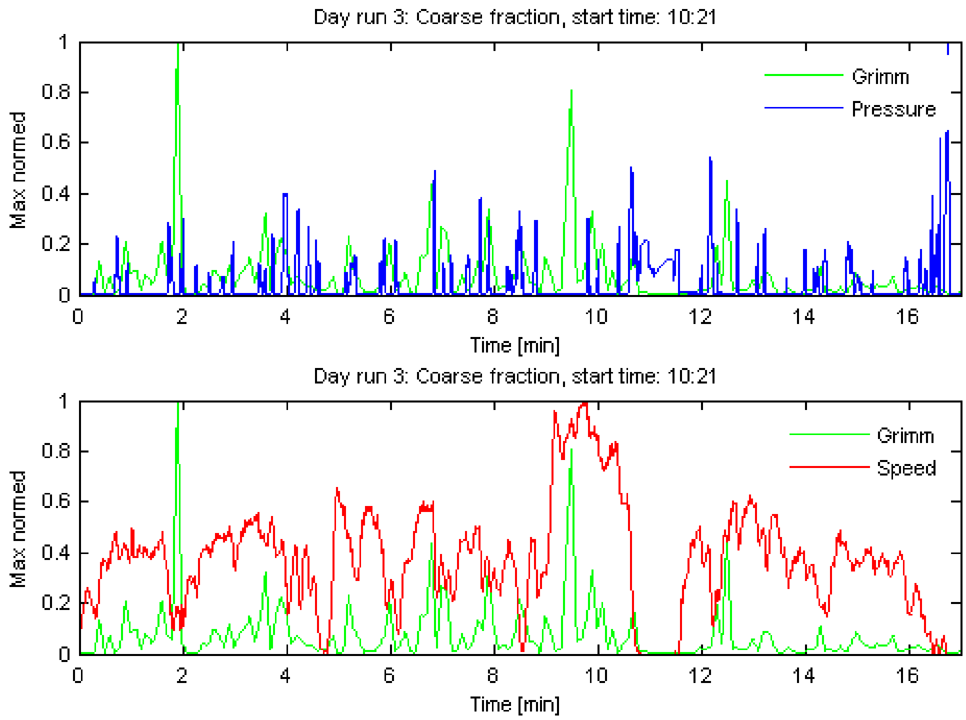

Figure 24. The green graph is the coarse fraction particle concentrations as measured by the GRIMM instrument, the blue graph is the measured brake cylinder pressure, and the red graph is the measured speed of the car.

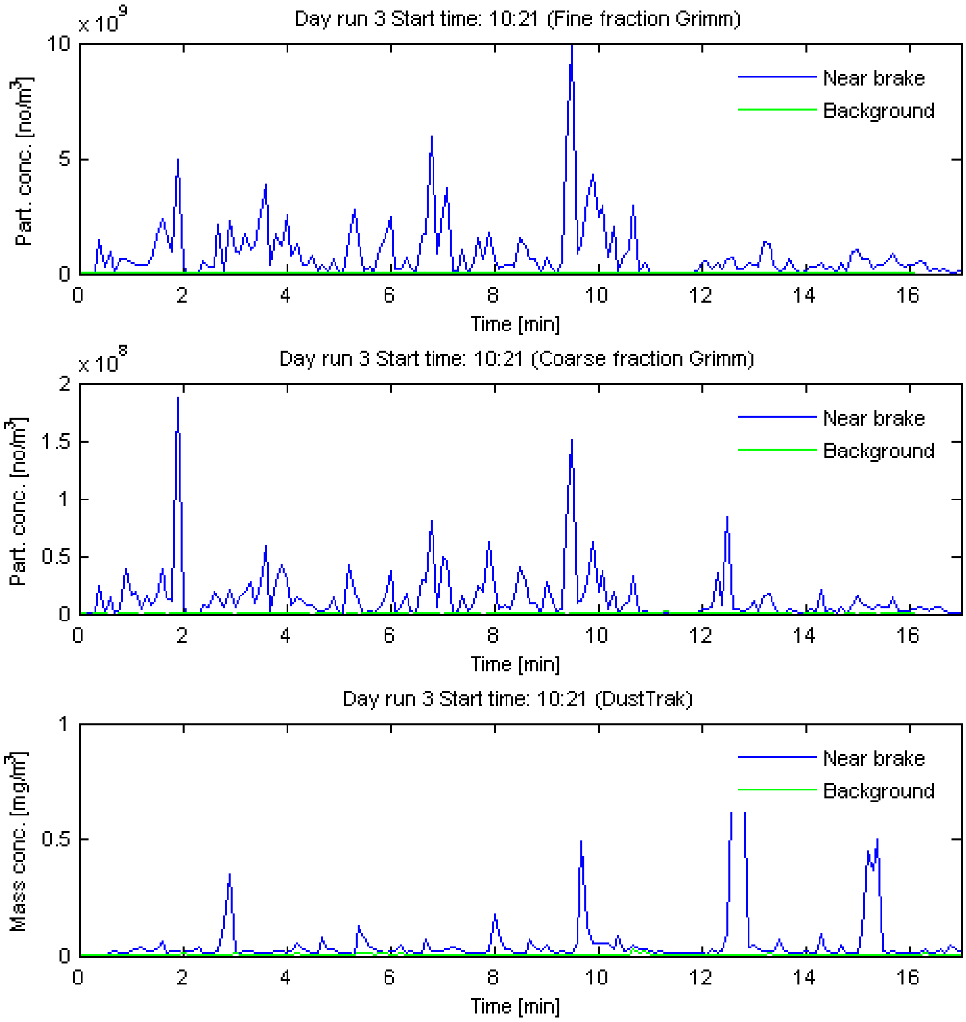

Figure 25. Fine and coarse fraction particle concentrations as measured by the GRIMM instrument during the test time and the mass concentration as measured by the DustTrak instrument. The blue graphs are the concentrations measured near the brake and the green graphs are the measured background concentration.

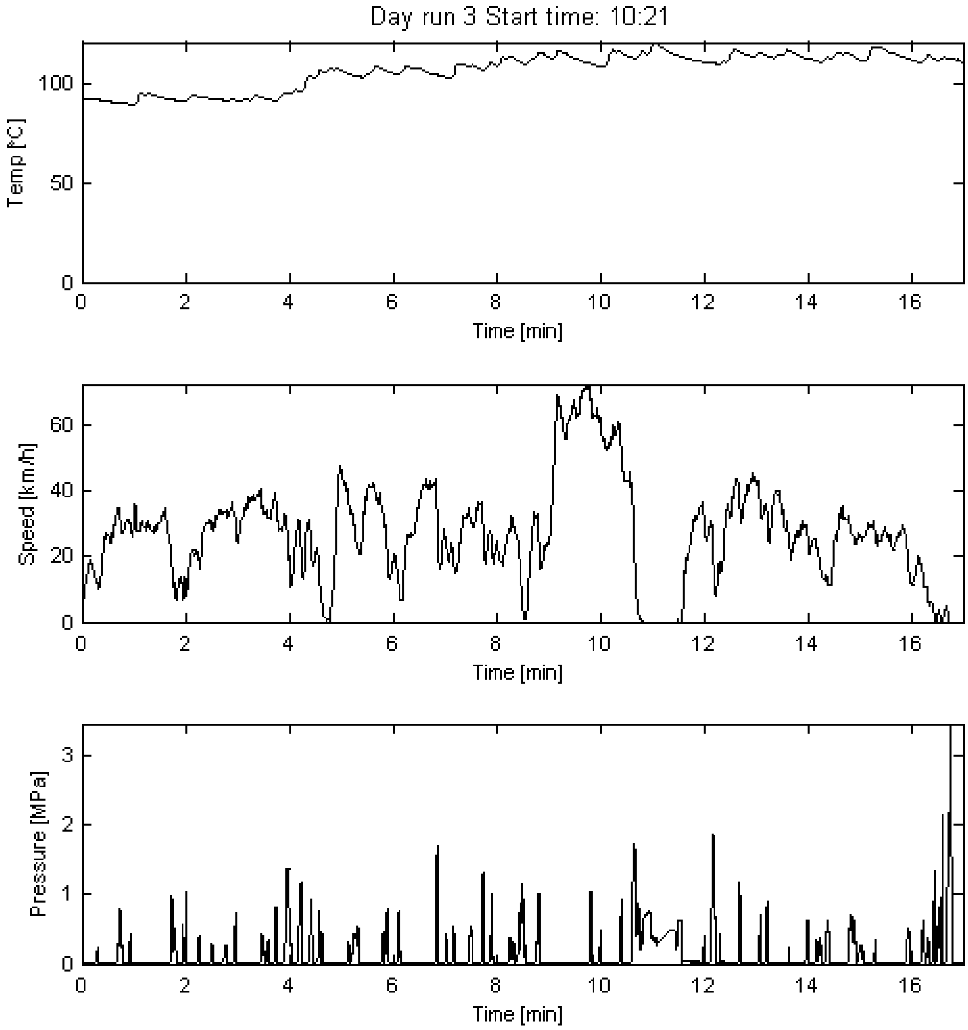

Figure 26. Finger side pad temperature, car speed and brake cylinder pressure measured during the test run.

7 Discussion

Some of the increases in particle concentration as measured by the Grimm can directly be correlated with an increase in brake cylinder pressure and a decrease in car speed, i.e. a brake event (Figure 8, Figure 12, Figure 16, Figure 20 and Figure 24). These increases were used to calculate the mean particle size distributions for the different test runs. All tests have a maximum peak in the mean particle size distribution, in the fine fraction, between 0.3 μm and 0.5 μm. This is similar to the results presented by Söderberg et al. [13] who tested brake pad materials in a pin-on-disc machine and measured brake wear particles online. Also, Wahlström et al. [14] used a disc brake assembly test stand where it is possible to measure the airborne wear particle distribution online. Mosleh et al [19] presented size distributions of wear particles collected on filters during pin-on-disc tests with brake materials at different testing conditions. In these three studies a peak in particle concentration occurred at about 0.35 μm which agrees with the results in this technical report. Sanders et al [10] conducted dynamometer and vehicle tests on pad materials, but these size distributions do not confirm the results in this report. They noted a peak in size distribution between 1 and 2 μm.

Not all of the increases in particle concentration correlate to brake events. Also, some car accelerations seem to correlate with an increase in particle concentration with may imply that resuspended road dust, tyre wear and or particles generated from pad to rotor dragging enters the test tubes near the brake. In all tests high levels in the measured particle concentration can be noticed between 9 and 11 minutes. There seems to be a local discharge of some aerosol in this area. One limitation of the test setup was problems with mist giving results indicating brake particle events. The reason was that the sampled air in the tubing from the front was heated by engine heat while transported to the instruments. This resulted in droplets drying up and water evaporating from particles falsely indicating fewer and smaller particles at the front than at the brake. There is need for similar temperature histories for brake and front particles.

None of the particle instruments measure actual particle geometry. In a future test series wear particles will be collected on filters for geometric analysis. Analysis of the particles trapped by these filters may also indicate, by comparison with particles collected on filters in test stands, that this test method measured brake wear particles. It would also be interesting to measure the amount of resuspended road dust during testing. In future testing it would also be interesting to measure to which extent the brake wear becomes airborne. This can be done by weighing the pads and rotor before and after the tests. It would also be of interest to test different type of brake pads in future testing.

The difference between the Grimm and the DustTrak instrument can be explained since DustTrak has a lower sensitivity for these kinds of particles. The particle size distribution (Figure 5) is similar for night run 2, day run 1 and day run 3. This can be explained by that the same physical particle instrument was used in these three measurements. Wahlström et al. [15] performed a test in heavy traffic with low relative air humidity and concluded that the particle concentration in the surrounding air couldn't be distinguished from the particle concentration measured near the brake. In the present work this is not a problem due to the difference in concentrations. Note that the mean particle concentration measured in the front of the car is not lower for the night time tests than for the day time tests which can be explained by the rainy weather in the day time runs.

The measured mean particle and mass concentration (Table 5) increases in following test runs, i.e. the concentration is higher in night run 2 than in night run 1 and day run 3 is higher than day run 2 etc. The particle and mass concentration measured in the front of the car (Table 4) don't follow this pattern. Note that the finger side pad temperature increases (Figure 10, Figure 14, Figure 18, Figure 22 and Figure 26) in following test runs. One interpretation of this is that more airborne particles are generated at higher temperatures of a brake. This result is in line with Wahlström et al. [14] and Sander et al. [10].

8 Conclusions

The results indicate that this test methodology can be used to measure the particle and mass concentration of airborne particles generated from a passenger car disc brake in traffic. The result also implies that improvements to the instrumentation can be done, for example mounting the test tubes in a way that the temperature do not differ between the tubes that go to the brake and to the front of the car. The particle- and volume-weighted mean particle diameter is 0.39 μm and 1.5 μm, respectively.

9 References

[1] Katsouyanni K, Touloumi G, Samoli E, Gryparis A, Le Tertre A, Monopolis Y, Rossi G, Zmirou D. Confounding and effect modification in the short-term effects of ambient particles on total mortality: results from 29 European cities within the APHEA2 project. *Epidemiology* 2001; **12(5)**: 521-531.

[2] Samet JM, Dominici F, Curriero FC, Coursac I, Zeger SL. Fine particulate air pollution and mortality in 20 U.S. cities 1987-1994. *N Engl J Med* 2000; **343(24)**: 1742-1749.

[3] Pope CA, Burnett RT, Thun MJ, Calle EE, Krewski D, Ito K, Thurston GD. Lung cancer, cardiopulmonary mortality, and long-term exposure to fine particulate air pollution. *JAMA* 2002; **287**: 1132-1141.

[4] Querol X, Alastuey A, Ruiz CR, Artiñano B, Hansson HC, Harrison RM, Buringh E, Ten Brink HM, Lutz M, Bruckmann P, Straeh P, Schneider J. Speciation and origin of PM10 and PM2.5 in selected European cities. *Atmospheric Environment* 2004; **38**: 6547–6555.

[5] Mahmoud Abu-Allaban, John A. Gillies, Alan W. Gertler, Russ Clayton, David Proffitt. Tailpipe, resuspended road dust, and brake-wear emission factors from on-road vehicles. *Atmospheric Environment* 2003; **37**: 5283–5293.

[6] Seaton A, Cherrie J, Dennekamp M, Donaldson K, Hurley J, Tran C. The London underground: dust and hazards to health. *Occup Environ Med* 2005; **62(6)**: 355–362.

[7] Branis M. The contributions of ambient sources to particle pollution in spaces and trains of the Prague underground transport system. *Atmospheric Environment* 2006; **40(2)**: 348–356.

[8] Abu-Allaban M, Gillies, JA, Gertler AW, Clayton R, Proffitt D. Tailpipe, resuspended road dust, and brake-wear emission factors from on-road vehicles. *Atmospheric Environment* 2003; **37(37)**: 5283–5293.

[9] Weckwerth G. Verification of traffic-emitted aerosol components in the ambient air of Cologne (Germany). *Atmospheric Environment* 2001; **35(32)**: 5525–5536.

[10] Sanders PG, Xu N, Dalka TM, Marico M. Airborne brake wear debris: size distributions, composition of dynamometer and vehicle test. *Environmental Science and Technology* 2003; **37(18)**: 4060–4069.

[11] Loug G, Schaur JJ, Soopark J, Shafer M, Deminter J, Weinstein J. Emission of metals associated with motor vehicle roadways. *Environmental Science and Technology* 2005; **39(3)**: 826–836.

[12] PJ Blau. Compositions, functions, and testing of friction brake materials and their additives. ORNL/TM-2001/64.

[13] Söderberg A, Wahlström J, Olander L, Jansson A, Olofsson U. On Airborne Wear Particles Emissions of Commercial Disc Brake Materials: A Pin on Disc Simulation. TRITA-MMK 2008:20 / ISSN 1400-1179 /ISRN/KTH/MMK/R-08/20-SE, Stockholm 2008.

[14] Wahlström J, Olander L, Olofsson U. Airborne Wear Particles Emissions of Commercial Disc Brake Materials – Disc Brake Test Stand Simulations at Low Contact Pressures and Rotors Pre-conditioned with Rust. TRITA-MMK 2008:16 / ISSN 1400-1179 /ISRN/KTH/MMK/R-08/16-SE, Stockholm 2008.

[15] Wahlström J, Söderberg A, Olander L, Jansson A , Olofsson U. Airborne Wear Particles from Passenger Car Disc Brakes - A Comparison of Measurements in Field Tests, Disc Brake Assembly Test Stand and Material Test Stand. Oral presentation at the SAE Brake Colloquium 2008. NR: 2008-01-2530.

[16] Peters TM, Ott D, O'Shaughnessy PT. Comparison of the Grimm 1.108 and 1.109 Portable Aerosol Spectrometer to the TSI 3321 Aerodynamic Particle Sizer for Dry Particles. *Annals of Occupational Hygiene* 2006; **50(8)**: 843–850.

[17] Liu Y, Daum PH. The effect of refractive index on size distributions and light scattering coefficients derived from optical particle counters. *Journal of Aerosol Science* 2000; **31(8)**: 945–957.

[18] Cheng YH. Comparison of the TSI Model 8520 and Grimm Series 1.108 portable aerosol instruments used to monitor particulate matter in an iron foundry. *Journal of Occupational and Environmental Hygiene* 2008; **5(3)**: 157–168.

[19] Mosleh M, Blau PJ, Dumitrescu D. Characteristics and morphology of wear particles from laboratory testing of disc brake materials. *Wear* 2004; **256(11-12)**: 1128-1134.